3-11-2010

Synthesis And Biological Evaluation Of Bupropion Analogues As Potential Pharmacotherapies For Smoking Cessation

F. Ivy Carroll

Bruce E. Blough

S. Wayne Mascarella

Hernan A. Navarro

J. Brek Eaton

See next page for additional authors

Authors

F. Ivy Carroll, Bruce E. Blough, S. Wayne Mascarella, Hernan A. Navarro, J. Brek Eaton, Ronald J. Lukas, and M. Imad Damaj

2204 J. Med. Chem. 2010, 53, 2204–2214
DOI: 10.1021/jm9017465

Journal of Medicinal Chemistry Article

Synthesis and Biological Evaluation of Bupropion Analogues as Potential Pharmacotherapies for Smoking Cessation

F. Ivy Carroll,*,† Bruce E. Blough,† S. Wayne Mascarella,† Hernán A. Navarro,† J. Brek Eaton,‡ Ronald J. Lukas,‡ and M. Imad Damaj§

†Center for Organic and Medicinal Chemistry, Research Triangle Institute, Research Triangle Park, North Carolina 27709-2194, ‡Division of Neurobiology, Barrow Neurological Institute, 350 West Thomas Road, Phoenix, Arizona 85013, and §Department of Pharmacology and Toxicology, Medical Campus, Virginia Commonwealth University, Richmond, Virginia 23219

Received November 25, 2009

Bupropion (**2a**) analogues were synthesized and tested for their ability to inhibit monoamine uptake and to antagonize the effects of human α3β4*, α4β2, α4β4, and α1* nAChRs. The analogues were evaluated for their ability to block nicotine-induced effects in four tests in mice. Nine analogues showed increased monoamine uptake inhibition. Similar to **2a**, all but one analogue show inhibition of nAChR function selective for human α3β4*-nAChR. Nine analogues have higher affinity at α3β4*-nAChRs than **2a**. Four analogues also had higher affinity for α4β2 nAChR. Analogues **2r**, **2m**, and **2n** with AD_{50} values of 0.014, 0.015, and 0.028 mg/kg were 87, 81, and 43 times more potent than **2a** in blocking nicotine-induced antinociception in the tail-flick test. Analogue **2x** with IC_{50} values of 31 and 180 nM for DA and NE, respectively, and with IC_{50} of 0.62 and 9.8 μm for antagonism of α3β4 and α4β2 nAChRs had the best overall in vitro profile relative to **2a**.

Introduction

Tobacco-related diseases remain as the predominant cause of premature mortality. An estimated one billion individuals worldwide are smokers.[1] Despite recent declines, it is estimated that 21% of the adult population in the U.S. are active smokers.[2] Since less than 10% of smokers are capable of quitting unaided, improvements in the clinical management of smoking are needed.[3]

Nicotine (**1**, Chart 1) is the main active ingredient in tobacco smoke that causes and maintains tobacco addiction. Nicotine produces a myriad of profound behavioral and physiological effects and is able to initiate and support drug-seeking behavior in humans and in laboratory animals.[4] The pharmacological and behavioral effects result from the activation of different nicotinic acetylcholine receptor (nAChR[a]) subtypes, which are members of an ionotropic neurotransmitter receptor superfamily.[5] nAChRs containing α4 and β2 or α7 subunits (α4β2- and α7-nAChR, respectively) are the two major subtypes found in the brain, although appreciable amounts of α3β4*- and α6β2*-nAChRs also are present in brain regions implicated in reward and drug dependence such as the substantia nigra, the ventral tegmental area (VTA), and the medial habenula system.[6−10]

Although nAChRs are the initial sites of action of nicotine in the brain, downstream events involving dopaminergic reward pathways may be critical in reinforcing smoking behavior. Nicotine, similar to other abused substances, is thought to be reinforcing because of the stimulation of mesolimbic dopamine reinforcement pathways.[11] Cigarette smoking acutely increases dopamine (DA) concentration in the ventral striatum/nucleus accumbens, key brain regions in the reward pathway.[12]

The first line medications on the market today to treat nicotine addiction are various nicotine replacement (NRT) formulations (nicotine gum, transdermal nicotine patches, vapor inhaler, nicotab, nasal spray, lozenges), presumed to mimic effects of tobacco-derived nicotine, the antidepressant bupropion (**2a**), and varenicline (**3**).[13] Both varenicline and bupropion SR (a sustained-release formulation) reduce symptoms of withdrawal, cigarette craving, and smoking reinforcement and produce smoking cessation with efficacy equal to or better than nicotine replacement.[14] However, none of these therapies has proven to be ideal, as smoking relapse still occurs at alarmingly high rates even after successful short-term therapies.

The use of **2a** for treating nicotine addiction resulted from serendipitous observations that patients taking **2a** as an antidepressant were more successful in smoking cessation attempts. It was known that **2a** inhibited DA and norepinephrine (NE) uptake activity, but the discovery that it also preferentially antagonized α3β4*-nAChR[15,16] suggested that more than one of these targets might be involved in its smoking cessation efficacy. It is possible that bupropion SR is achieving its effects by increasing dopamine levels through DA uptake inhibition and shielding against nicotine induction of nAChR-mediated dopamine elevation. Although it is not clear what part if any is played by the ability of **2a** to inhibit NE uptake in its smoking cessation activity, it is likely to contribute to nicotine withdrawal amelioration. Surprisingly, very little effort has been devoted toward the development of **2a** analogues with improved smoking cessation properties.[17−19]

*To whom correspondence should be addressed. Telephone: 919-541-6679. Fax: 919-541-8868. E-mail: fic@rti.org.

[a]Abbreviations: DA, dopamine; 5HT, serotonin; NE, norepinephrine; SR, sustained release; HEK, human embryonic kidney; DAT, dopamine transporter; SERT, serotonin transporter; NET, norepinephrine transporter; nAChR, nicotinic acetylcholine receptor; VTA, ventral tegmental area; NRT, nicotine replacement therapy; CTDP, Cocaine Treatment Discovery Program; NIDA, National Institute on Drug Abuse; MPE, maximum possible effect.

 Published on Web 02/16/2010

Chart 1

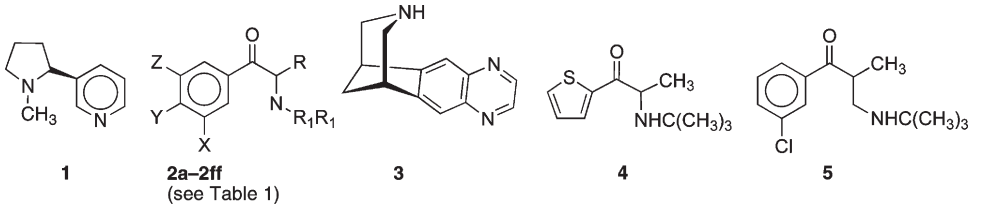

Scheme 1[a]

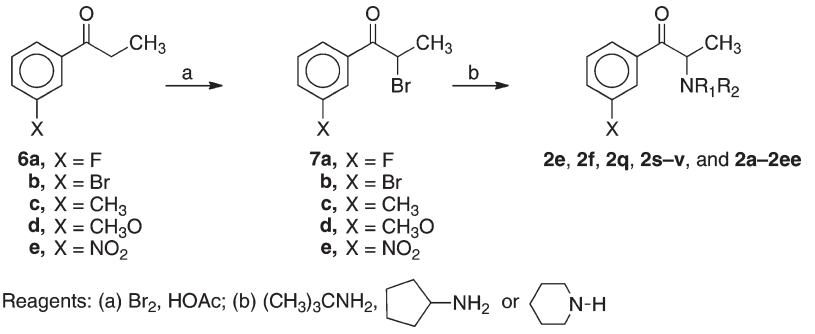

Compound **2a** inhibits DA reuptake, increasing the synaptic levels of DA. Compound **2a** also inhibits nicotine-induced DA and NE overflow from superfused striatial and hippocampal slices, respectively.[20] Thus, **2a** might be functioning as an indirect DA agonist by reward modulation of this downstream action of nicotine. The ability of **2a** to alleviate withdrawal symptoms is consistent with an indirect dopamine agonist mechanism.[21,22] Compound **2a** noncompetitively inhibits carbamylcholine-induced $^{86}Rb^{+}$ efflux from human neuroblastoma cells expressing $\alpha3\beta4$*-nAChR[15] and function of $\alpha3\beta2$-, $\alpha4\beta2$-, and $\alpha7$-nAChR heterologously expressed in Xenopus oocytes.[16] Other studies suggest that $\alpha3\beta4$*-nAChR plays a major role in nicotine-evoked NE release from hippocampus.[23,24]

We recently reported the synthesis of a number of **2a** analogues that were evaluated for their abilities to inhibit neurotransmitter uptake by the dopamine, norepinephrine, or serotonin (5HT) transporters, DAT, NET, or SERT, respectively, under the National Institute on Drug Abuse (NIDA) Cocaine Treatment Discovery Program (CTDP).[25] Those studies sought to identify entities with better potency and selectivity toward DAT than **2a** and whose activity as an indirect dopamine agonist might reveal a novel pharmacotherapy for treating cocaine addiction. In the current study, we designed and developed **2a** analogues as smoking cessation aids, seeking entities that possess increased inhibitory activity for DA and NE uptake inhibition and/or nAChR antagonism while retaining the druglike properties of the lead compound. In this study we report the synthesis and biological evaluation of **2a** analogues **2b**−**ff**, **4**, and **5**. Some of the analogues have higher inhibitory potencies than **2a** at DAT and NET as well as at $\alpha3\beta4$*-nAChR. In addition, some of the compounds antagonize the antinociceptive, hyperlocomotor, and hypothermic effects of acutely administered nicotine in mice with potencies greater than that of **2a**. 2-(*N*-*tert*-Butylamino)-3′,4-dichloropentanophenone (**2x**), which was 41- and 7.5-fold more potent in inhibition of DA and NE uptake and 3-fold more potent as an $\alpha3\beta4$*-nAChR antagonist than **2a**, is one of the more interesting compounds. Compound **2x** is also 9 times more potent than **2a** as an antagonist of nicotine-induced antinociception in the mouse tail-flick test.

Chemistry

The **2a** analogues **2b**−**d**, **2g**−**p**, **2r**, **2w**−**z**, **2ff**, **4**, and **5** were synthesized as previously reported.[25] The new **2a** analogues **2e**, **2f**, **2q**, **2s**−**v**, and **2aa**−**ee** were prepared using procedures exactly analogous to those used to synthesize the reported analogues. Thus, bromination of the ketones **6a**−**e** with bromine in acetic acid afforded the bromoketones **7a**−**e** (Scheme 1). Treatment of **7a**−**e** with *tert*-butylamine, cyclopentylamine, and piperidine yielded the desired **2a** analogues **2e**, **2f**, **2q**, **2s**−**v**, **2aa**−**ee**, **4**, and **5**.

In Vitro Assays. The **2a** analogues **2b**−**ff**, **4**, and **5** were evaluated for their ability to block reuptake of [^{3}H]dopamine ([^{3}H]DA), [^{3}H]serotonin ([^{3}H]5HT), and [^{3}H]norepinephrine ([^{3}H]NE) using (h)DAT, (h)SERT, and h(NET) stably expressed in HEK293 cells using conditions similar to those previously reported.[26,27] The results are given in Table 1. [^{3}H]DA, [^{3}H]5HT, and [^{3}H]NE uptake values for **2a** and analogues **2b**−**d**, **2g**−**p**, **2r**, and **2n**−**z** were obtained as a part of the NIDA CTDP and previously reported.[25] For the most part, the relative potency in both evaluations was the same. However, in general, the efficacy in this study tended to be higher (lower IC_{50} values) for all analogues than the efficacies obtained in the CTDP program.[25] There were some exceptions. For example, in the case of **2o**, we obtained IC_{50} values of 209, 607, and 16 000 nM for the inhibition of [^{3}H]DA, [^{3}H]SERT, and [^{3}H]NE uptake compared to 31 and 969 nM and inactive in the CTDP program.

Compound **2a** analogues **2b**−**ff**, **4**, and **5** were also evaluated for their ability to antagonize functional responses of $\alpha3\beta4$*-, $\alpha4\beta2$-, $\alpha4\beta4$-, and $\alpha1$*-nAChR using previously reported methods[27] modified as described in Experimental Section. Results are given in Table 1 and in Figures 1 and 2.[27]

In Vivo Assays. Compound **2a** and analogues **2b**−**ff**, **4**, and **5** were also evaluated for their ability to antagonize behavioral responses to acute nicotine administration as previously described.[27] Results are given in Table 2.

Results

Compound **2a** and its analogues were evaluated for their ability to inhibit DA, NE, and 5-HT uptake inhibition using

Table 1. Analogue Inhibition of Monoamine Uptake and Nicotinic Acetylcholine Receptor (nAChR) Function

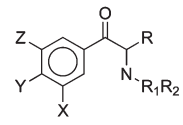

2a-2ff

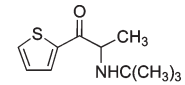

4

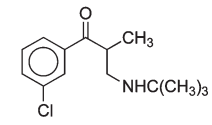

5

							monoamine uptake inhibition[a] IC$_{50}$ (nM)			nAChR inhibition[b] IC$_{50}$ (μM)			
compd	R	R$_1$	R$_2$	X	Y	Z	[^{3}H]DA	[^{3}H]NE	[^{3}H]SERT	$\alpha3\beta4$*-	$\alpha4\beta2$-	$\alpha4\beta4$-	$\alpha1$*-
2a	CH_3	H	$C(CH_3)_3$	Cl	H	H	658 ± 178	1850 ± 300	IA	1.8 (1.15)	12 (1.15)	15 (1.07)	7.9 (1.12)
2b	CH_3	H	$C(CH_3)_3$	F	H	H	2320 ± 860	6500 ± 270	IA	4.4 (1.07)	21 (1.12)	52 (1.07)	32 (1.07)
2c	CH_3	H	$C(CH_3)_3$	Br	H	H	511 ± 33	5600 ± 1300	IA	1.3 (1.07)	15 (1.12)	13 (1.15)	10 (1.07)
2d	CH_3	H	$C(CH_3)_3$	CH_3	H	H	1470 ± 170	6200 ± 3500	IA	1.5 (1.07)	19 (1.07)	17 (1.15)	11 (1.07)
2e	CH_3	H	$C(CH_3)_3$	CH_3O	H	H	3620 ± 460	IA	IA	2.0 (1.05)	37 (1.07)	23 (1.10)	16 (1.15)
2f	CH_3	H	$C(CH_3)_3$	NO_2	H	H	IA	IA	IA	11 (1.07)	36 (1.10)	74 (1.07)	41 (1.12)
2g	CH_3	H	$C(CH_3)_3$	H	Cl	H	1090 ± 150	2070 ± 660	9800 ± 4700	2.4 (1.10)	33 (1.12)	18 (1.15)	14 (1.07)
2h	CH_3	H	$C(CH_3)_3$	H	Br	H	689 ± 229	2540 ± 740	4508 ± 1722	1.4 (1.07)	23 (1.10)	13 (1.15)	7.6 (1.07)
2i	CH_3	H	$C(CH_3)_3$	H	CH_3	H	1950 ± 390	2350 ± 560	IA	2.4 (1.10)	17 (1.07)	16 (1.29)	12 (1.15)
2j	CH_3	H	$C(CH_3)_3$	F	F	H	7978 ± 4437	6480 ± 2100	IA	2.6 (1.10)	45 (1.12)	40 (1.35)	24 (1.07)
2k	CH_3	H	$C(CH_3)_3$	Cl	Cl	H	463 ± 104	1670 ± 250	8800 ± 1030	6.8 (1.07)	29 (1.10)	12 (1.15)	9.8 (1.10)
2l	CH_3	H	$C(CH_3)_3$	Cl	CH_3	H	410 ± 75	2040 ± 280	IA	0.65 (1.10)	9.2 (1.07)	4.8 (1.15)	5.7 (1.07)
2m	CH_3	H	$C(CH_3)_3$	CH_3	Br	H	2810 ± 590	7250 ± 2370	IA	2.9 (1.07)	32 (1.10)	18 (1.20)	12 (1.07)
2n	CH_3	H	$C(CH_3)_3$	Cl	H	Cl	IA	14000 ± 4700	IA	3.1 (1.12)	19 (1.10)	22 (1.35)	17 (1.10)
2o	C_2H_5	H	$C(CH_3)_3$	Cl	H	H	209 ± 28	607 ± 190	16000 ± 6700	0.58 (1.23)	8.6 (1.05)	6.2 (1.26)	3.9 (1.07)
2p	C_3H_7	H	$C(CH_3)_3$	Cl	H	H	56 ± 18	370 ± 80	IA	0.70 (1.17)	7.7 (1.07)	4.9 (1.20)	2.0 (1.07)
2q	CH_3	H	$CH(CH_2CH_2CH_2CH_2)$	F	H	H	693 ± 270	2850 ± 520	IA	11 (1.07)	81 (1.15)	IA	26 (1.07)
2r	CH_3	H	$CH(CH_2CH_2CH_2CH_2)$	Cl	H	H	IA	IA	IA	26 (1.10)	IA	IA	IA
2s	CH_3	H	$CH(CH_2CH_2CH_2CH_2)$	Br	H	H	845 ± 120	2530 ± 930	IA	3.9 (1.07)	42 (1.15)	27 (1.07)	6.5 (1.07)
2t	CH_3	H	$CH(CH_2CH_2CH_2CH_2)$	CH_3	H	H	842 ± 190	8700 ± 3200	IA	3.7 (1.10)	25 (1.05)	23 (1.10)	5.8 (1.10)
2u	CH_3	H	$CH(CH_2CH_2CH_2CH_2)$	CH_3O	H	H	2270 ± 330	8200 ± 2370	6900 ±	4.7 (1.07)	31 (1.10)	46 (1.07)	9.2 (1.07)
2v	CH_3	H	$CH(CH_2CH_2CH_2CH_2)$	NO_2	H	H	IA	IA	IA	15 (1.05)	IA	60 (1.07)	19 (1.10)
2w	C_2H_5	H	$C(CH_3)_3$	Cl	Cl	H	118 ± 40	389 ± 83	1090 ± 480	0.51 (1.20)	10 (1.07)	3.3 (1.17)	2.7 (1.07)
2x	C_3H_7	H	$C(CH_3)_3$	Cl	Cl	H	31 ± 9.4	180 ± 69	2300 ± 370	0.62 (1.29)	9.8 (1.07)	4.2 (1.20)	1.5 (1.12)
2y	CH_3	CH_3	$C(CH_3)_3$	Cl	H	H	6000 ± 316	1570 ± 80	IA	1.2 (1.20)	IA	16 (1.23)	16 (1.10)
2z	CH_3	CH_3	CH_3	Cl	H	H	1750 ± 370	1520 ± 250	IA	37 (1.12)	IA	33 (1.23)	IA
2aa	CH_3	$CH_2CH_2CH_2CH_2CH_2$		F	H	H	156 ± 46	135 ± 36	IA	35 (1.07)	71 (1.66)	IA	IA
2bb	CH_3	$CH_2CH_2CH_2CH_2CH_2$		Br	H	H	750 ± 173	1180 ± 270	IA	11 (1.07)	74 (1.15)	64 (1.05)	19 (1.07)
2cc	CH_3	$CH_2CH_2CH_2CH_2CH_2$		CH_3	H	H	414 ± 89	577 ± 61	IA	11 (1.10)	56 (1.10)	IA	53 (1.10)
2dd	CH_3	$CH_2CH_2CH_2CH_2CH_2$		CH_3O	H	H	452 ± 82	718 ± 130	IA	16 (1.10)	57 (1.10)	IA	87 (1.10)
2ee	CH_3	$CH_2CH_2CH_2CH_2CH_2$		NO_2	H	H	10000 ± 1900	4100 ± 540	IA	53 (1.10)	IA	IA	IA
2ff	CH_3	$CH_2CH_2CH_2CH_2CH_2$		Cl	H	H	852 ± 220	2520 ± 900	IA	7.7 (1.12)	30 (1.12)	83 (1.23)	28 (1.07)
4							IA	IA	IA	10 (1.12)	32 (1.10)	IA	69 (1.07)
5							IA	IA	IA	3.3 (1.17)	35 (1.05)	36 (1.23)	16 (1.05)

[a] Values for mean ± standard error of three independent experiments, each conducted with triplicate determination. [b] Mean micromolar IC$_{50}$ values (to 2 significant digits) for **2a** and the indicated analogues from three independent experiments for inhibition of functional responses to an EC$_{80}$−EC$_{90}$ concentration of carbamylcholine mediated by nAChR subtypes composed of the indicated subunits (where the asterisk (*) indicates that additional subunits are or may be additional assembly partners with the subunits specified; see Experimental Section). Numbers in parentheses indicate SEM as a multiplication/division factor of the mean micromolar IC$_{50}$ values shown [i.e., the value 1.8 (1.15) reflects a mean IC$_{50}$ value of 1.8 μM with an SEM range of 1.8 × 1.15 μM to 1.8/1.15 μM or 1.6−2.1 μM. IA: IC$_{50}$ > 100 μM.

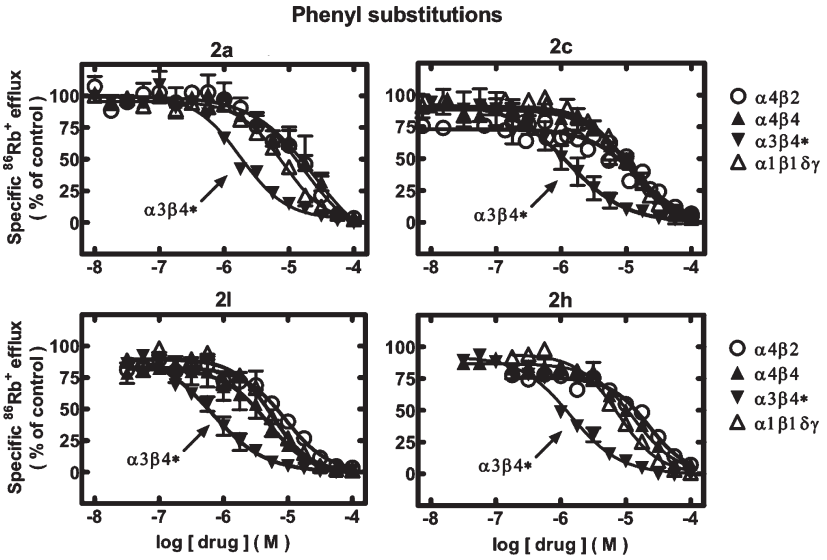

Figure 1. Specific $^{86}Rb^+$ efflux (ordinate, percentage of control) was determined for functional, human muscle-type $\alpha 1\beta 1\gamma\delta$-nAChR (△), ganglionic $\alpha 3\beta 4$*-nAChR (▼), $\alpha 4\beta 2$-nAChR (○), or $\alpha 4\beta 4$-nAChR (▲) naturally or heterologously expressed in human cell lines in the presence of a receptor subtype-specific, $EC_{80}-EC_{90}$ concentration of the full agonist, carbamylcholine, either alone or in the presence of the indicated concentrations (abscissa, log molar) of **2a** or its analogues having phenyl substitutions (compounds **2c**, **2l**, and **2h**) as indicated. Mean micromolar IC_{50} values and SEM as a multiplication/division factor of the mean micromolar IC_{50} value are provided in Table 1.

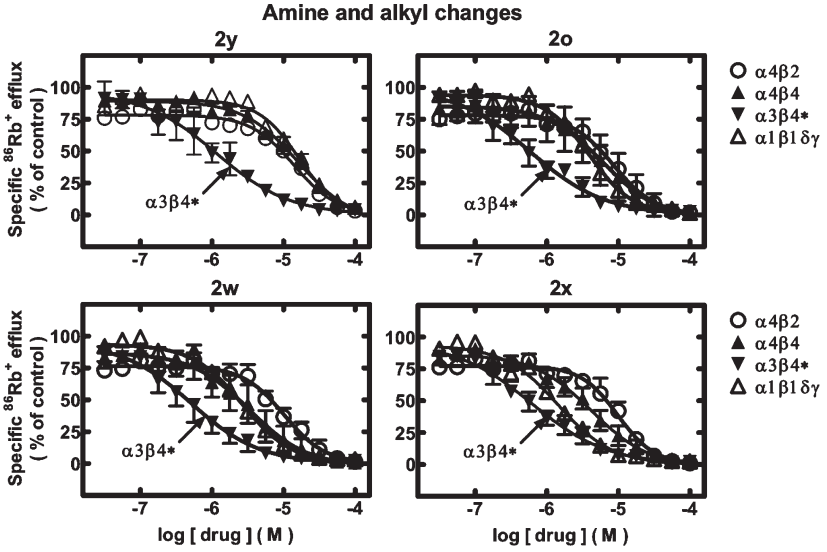

Figure 2. Specific $^{86}Rb^+$ efflux (ordinate, percentage of control) was determined for functional, human muscle-type $\alpha 1\beta 1\gamma\delta$-nAChR (Δ), ganglionic $\alpha 3\beta 4$*-nAChR (▼), $\alpha 4\beta 2$-nAChR (○), or $\alpha 4\beta 4$-nAChR (▲) naturally or heterologously expressed in human cell lines in the presence of a receptor subtype-specific, $EC_{80}-EC_{90}$ concentration of the full agonist, carbamylcholine, either alone or in the presence of the indicated concentrations (abscissa, log molar) of **2a** analogues having alkyl or phenyl plus alkyl substitutions (compounds **2y**, **2o**, **2w**, and **2x**) as indicated. Mean micromolar IC_{50} values and SEM as a multiplication/division factor of the mean micromolar IC_{50} value are provided in Table 1.

human DAT, NET, and SERT homologously expressed by HEK293 cells. Compound **2a** has IC_{50} values of 658 and 1850 nM for inhibition of DA and NE uptake, respectively, and is inactive at SERT (Table 1). Very few **2a** analogues had appreciably better IC_{50} values for DA uptake inhibition than **2a**. Compounds **2o** and **2p**, where the α-methyl group in **2a** was replaced by ethyl and propyl groups, respectively, have IC_{50} values for inhibition of DA uptake of 209 and 56 nM, respectively, indicating that replacement of the α-methyl group with larger alkyl chains produced ligands with better efficacy, a finding that also is borne out by the improvement in inhibitory potency at DAT for **2w** (IC_{50} = 118 nM) and **2x** (IC_{50} = 31 nM) relative to **2k** (IC_{50} = 463 nM) in the 3,4-dichlorophenyl analogue group. In each case, the 3,4-dichlorophenyl analogue has higher inhibitory potency for DA uptake inhibition than the otherwise equivalent monochlorophenyl analogue. Each 3,4-dichlorophenyl compound (**2k**, **2w**, **2x**) also has slightly better inhibitory potency for NE uptake (1670, 389, and 180 nM IC_{50} values, respectively) greater than the equivalent monochlorophenyl compounds (**2a**, **2o**, **2p**; 1850, 607, 370 nM IC_{50} values, respectively). The propyl **2a** analogue (**2p**) and 3,4-dichlorophenyl propyl analogue **2x** have 7- and 6-fold selectivity for DA over NE uptake inhibition.

Compound **2aa** has 4- and 14-fold elevated inhibitory potency relative to **2a** for DA uptake inhibition (IC_{50} = 156 nM) and NE uptake inhibition (IC_{50} = 135 nM). Compound **2y** is the only compound tested that has higher selectivity

Table 2. Pharmacological Evaluation of **2a** Analogues as Noncompetitive Nicotinic Antagonists[a]

	AD_{50} (mg/kg)			
compd	tail-flick	hot-plate	locomotion	hypothermia
2a	1.2 (1−1.8)	15 (6−19)	4.9 (0.9−46)	9.2 (4−23)
2b	IA	IA	IA	IA
2c	0.12 (0.03−0.5)	14.9 (6.5−34)	27.1 (2.9−46)	11.5 (8.2−16.1)
2d	0.05 (0.03−0.2)	6.8 (4.2−11.1)	4.3 (0.7−28)	7.8 (7.4−8.2)
2e	1.6 (0.4−5.4)	IA	IA	IA
2f	IA	IA	IA	IA
2g	0.43 (0.08−2.3)	IA	31 (12.8−74.2)	32 (10.1−100.1)
2h	0.15 (0.04−0.6)	23.5 (12.3−44.6)	IA	29 (11.8−69.1)
2i	0.09 (0.03−0.9)	7.75 (2.8−21)	11.8 (5.8−23)	8.8 (2−38.2)
2j	0.05 (0.02−0.11)	IA	IA	IA
2k	0.28 (0.08−0.9)	IA	IA	IA
2l	0.2 (0.13−1.3)	7.2 (0.13−13)	11 (1.5−83)	10 (5.1−18.2)
2m	0.015 (0.005−0.04)	IA	IA	IA
2n	0.028 (0.01−0.07)	4.3 (0.2−13.5)	IA	IA
2o	0.5 (0.1−2.1)	IA	11.7	IA
2p	10 (3.7−26)	IA	IA	IA
2q	IA	IA	IA	IA
2r	0.014 (0.001−0.08)	IA	IA	IA
2s	IA	IA	IA	IA
2t	IA	IA	IA	IA
2u	IA	IA	IA	IA
2v	na	na	na	na
2w	0.05 (0.03−0.8)	IA	IA	IA
2x	0.13 (0.06−0.3)	15 (0.9−25)	IA	17.5 (13−24)
2y	0.46 (0.44−0.48)	8.7 (2−37)	IA	IA
2z	5.2 (1.5−17.2)	IA	IA	IA
2aa	3.84 (3.3−4.4)	IA	IA	7.5 (2.4−24)
2bb	IA	IA	IA	IA
2cc	IA	IA	IA	IA
2dd	4.5 (1.4−14.3)	IA	IA	IA
2ee	IA	IA	IA	IA
2ff	0.05 (0.005−0.5)	IA	IA	IA
4	0.077 (0.015−0.4)	IA	IA	IA
5	10.5 (9.5−11.5)	IA	IA	16 (9.3−26)

[a] Results are expressed as AD_{50} (mg/kg) ± confidence limits (CL) or % effect at the highest dose tested. Dose−response curves were determined using a minimum of four different doses of test compound, and at least eight mice were used per dose group. IA: $IC_{50} > 100\ \mu M$. na: not assayed.

(~4-fold) for NE uptake inhibition relative to DA inhibition, but it is only marginally more potent as an NE uptake inhibitor than **2a** (IC_{50} of 1570 and 1850 nM, respectively). None of these analogues has IC_{50} values for inhibition of SERT less than 1 μM, although the dichlorophenyl analogues are more potent at this target than their monochlorophenyl equivalents.

Thus, **2w**, **2x**, and **2p** are the most potent for DA uptake inhibition, with **2aa** and **2o** also being more potent for DA uptake inhibition than **2a**. Compounds **2w** and **2x** also are more selective for DA uptake inhibition relative to inhibitions of 5-HT and NE uptake. Compounds **2aa**, **2x**, and **2p** are the most potent analogues for NE uptake inhibition, and analogues **2w**, **2o**, and **2dd** are also more potent than **2a** for NE uptake inhibition. With the exception of **2y**, which is about 4-fold selective for NE over DA uptake inhibition uptake inhibition (although being about equipotent with **2a** at NET), none of the analogues is selective for NE over DA uptake inhibition.

Isotopic $^{86}Rb^+$ efflux assays were used to determine effects of **2a** and analogues on function of diverse human nAChR subtypes naturally or heterologously expressed by human cell lines. These assays repeatedly have been shown to be specific only for nAChR function in the cells used. In the case of SH-SY5Y cells, function of only $\alpha3\beta4$*-nAChR is measured because $\alpha7$-nAChRs that also are expressed by these cells activate and inactivate too quickly to detectably contribute to ion flux. Neither **2a** nor any of the analogues tested possess intrinsic activity as agonists at $\alpha1$*-, $\alpha3\beta4$*-, $\alpha4\beta2$-, or $\alpha4\beta4$-nAChR. $^{86}Rb^+$ efflux in the presence of these ligands alone at concentrations from ~5 nM to 100 μM (data not shown here) was indistinguishable from responses in cells exposed only to efflux buffer.

$^{86}Rb^+$ efflux assays also were used to assess whether **2a** or its analogues had activity as antagonists at human nAChR. With few exceptions (noted in Table 1), **2a** and each of its analogues exhibited concentration-dependent inhibition of ion flux responses elicited by $EC_{80}-EC_{90}$ concentrations of carbamylcholine for $\alpha1$*-, $\alpha3\beta4$*-, $\alpha4\beta2$-, and $\alpha4\beta4$-nAChR. Representative concentration response curves for **2a** itself, for compounds having substituted phenyl groups (**2c**, **2h**, **2l**; Figure 1), or for compounds having amine or alkyl charges (**2y**, **2o**, **2x**, **2w**; Figure 2) illustrate some of the features of these ligands (see also Table 1).

Compound **2a** has IC_{50} values of 1.8, 12, 15, and 7.9 μM for $\alpha3\beta4$*-, $\alpha4\beta2$-, $\alpha4\beta4$-, and $\alpha1$*-nAChRs, respectively, and thus is 4- to 8-fold selective for the $\alpha3\beta4$* relative to the other nAChRs. All of the analogues except **2z** (approximately equipotent at $\alpha3\beta4$*- and $\alpha4\beta4$-nAChR) block function of $\alpha3\beta4$*-nAChR at concentrations lower than those needed to inhibit function of the other nAChR subtypes. That is, all of the analogues are selective in their antagonism for $\alpha3\beta4$*-nAChR. Compounds **2l**, **2o**, **2p**, and **2x** have slightly higher potencies than **2a**, the $\alpha4\beta2$ nAChR (IC_{50} = 7.7−9.8 μm).

The 4-fold selectivity of **2a** for the α3β4*-nAChR over other subtypes is increased to >7-fold for the 3-bromo, 3-methyl, and 3-methoxyphenyl analogues **2c**, **2d**, and **2e**, respectively, and to >10-fold for the 3,4-difluorophenyl and *N*-methyl analogues **2j** and **2y**, respectively.

In addition to the improvements in selectivity for α3β4*-nAChR over other subtypes, the 3-chloro, 4-methyl substituted phenyl analogue **2l** (IC_{50} = 0.65 μM) has ~3-fold higher inhibitory potency at α3β4*-nAChR relative to **2a**. Both mono- and dichloro-substituted phenyl compounds **2o**, **2p**, **2w**, and **2x** (IC_{50} = 0.51−0.70 μM), having extended alkyl side chains, have ~3-fold higher potency at α3β4*-nAChR relative to **2a** with the 3,4-dichlorophenyl ethyl and propyl compounds (**2w** and **2x**), respectively, being >10-fold more potent than the unextended 3,4-dichlorophenyl analogue (**2k**; IC_{50} = 6.8 μM). These compounds also are remarkable because they also had higher inhibitory potency at and selectivity for DA uptake inhibition and higher potency for NE uptake inhibition than **2a**, so they all represent analogues with higher affinity than **2a** for three of its molecular targets.

Compound **2a** blocks nicotine-induced antinociception in the tail-flick and hot-plate tests with AD_{50} values of 1.2 and 15 mg/kg, respectively (Table 2). It also blocks nicotine-induced locomotor activity and hypothermia with AD_{50} values of 4.9 and 9.2 mg/kg, respectively. Seventeen of the 33 analogues had AD_{50} values of 0.014−0.5 mg/kg in the tail-flick test, showing higher inhibitory potency than **2a**. Analogues **2r**, **2m**, and **2n** with AD_{50} values of 0.014, 0.015, and 0.028 mg/kg were 86, 80, and 43 times more potent than **2a** in blocking nicotine-induced antinociception in the tail-flick test. Surprisingly, none of these analogues has higher potency than **2a** for DA, NE, and SERT uptake inhibition or any nAChR subtype. Analogues **2d**, **2j**, **2w**, and **2ff** with AD values of 0.05 mg/kg were the next most potent in the tail-flick assay, being 24-fold more potent than **2a**. Analogues **2c**, **2h**, **2i**, and **2x** (AD_{50} = 0.09−0.15 mg/kg) have ~10-fold better inhibitory potency than **2a** against nicotine-mediated analgesia in the tail-flick assay. Thus, **2x** is an analogue that has increased potency relative to **2a** as an inhibitor of DA and NE uptake, and at α3β4*-nAChR, analogues **2h** and **2c** have potencies comparable to those of **2a** across those targets. The 3,4-dichlorophenyl analogues **2k**, **2w**, and **2x** are ~4-, ~10-, and ~77-fold more potent than their 3-chlorophenyl substituted equivalents **2a**, **2o**, and **2p**, respectively. However, the tail-flick assay results are not particularly illuminating about the molecular targets contributing to analogue effects, perhaps because effects at higher levels might override the presumed spinal level of nicotine-mediated antinociception.

In the hot-plate assay, **2d** and **2l** (potent and selective at α3β4*-nAChR) and **2y** (selective for NE uptake inhibition and α3β4*-nAChR) have about 2-fold more potency than **2a**, and **2n** (inactive at transporters and less potent than **2a** at α3β4*-nAChR) has about 3-fold more potency. These findings suggest that several mechanisms might impact supraspinal mechanisms of nicotine-mediated antinociception.

Of all the analogues, only **2d** has potency like **2a** in blocking nicotine's effects on locomotion, and only **2d** and **2l** rival the ability of **2a** to inhibit nicotine's effects on body temperature. Similar to **2a**, substituted phenyl analogues **2c**, **2d**, and **2l** (roughly sharing the in vitro fingerprint of **2a**) had potency in all four behavioral tests as nicotine antagonists. Compound **2x**, a potent DA and NE uptake inhibitor and α3β4*-nAChR antagonist, had potency in three of four of the in vivo tests.

Compounds **2p**, **2w**, and **2x**, having the highest potencies as DA uptake inhibitors, differ nearly 200-fold in potency in the tail-flick assay, and only **2x** shows activity in the hot-plate or locomotor tests. These analogues also are among the most potent at NE uptake inhibition.

Discussion

Several **2a** analogues were synthesized and tested for their ability to inhibit monoamine uptake and to antagonize function of four different nAChR subtypes. The analogues were also evaluated for their ability to block nicotine-induced antinociception, locomotor activity, and hypothermia.

We succeeded in creating and characterizing analogues with significantly lower IC_{50} values relative to **2a** for inhibition of both DA or NE uptake inhibition (**2o**, **2p**, **2w**, **2x**, and **2aa**).

The current efforts also succeeded in generating nine agents with higher (**2l**, **2o**, **2p**, **2w**, **2x**) or slightly higher (**2c**, **2d**, **2h**, **2y**) antagonist potency relative to **2a** at α3β4*-nAChR. Of these, **2c**, **2d**, **2l**, and especially **2y** also have improved selectivity for α3β4*-nAChR over other nAChR subtypes relative to **2a**. In addition, analogues **2e** and **2j** show improved selectivity for α3β4*-nAChR although without having lower IC_{50} values than **2a**.

Compounds were also developed that had altered target selectivity between nAChR and transporters. For example, **2e** had improved selectivity for α3β4*-nAChR over DA and NE uptake inhibition, **2y** improved selectivity for α3β4*-nAChR over DA uptake inhibition, and **2p**, **2w**, and **2x** improved selectivity for DA and NE uptake inhibition over α3β4*-nAChR antagonism relative to **2a**.

Thus, several new compounds have been developed that have higher potency and/or selectivity at specific neurotransmitter transporters or α3β4*-nAChR than **2a**, thereby providing leads for further target-directed drug development. These compounds also afford, in principle, opportunities to dissect roles of specific molecular targets in nicotine-mediated behavioral effects. Structure−activity relationships are complex and difficult to generalize because phenyl substitutions and amine/alkyl changes seem to interact in terms of altering potencies at and selectivities for specific targets in vitro. However, compounds with alkyl chain extensions in monochlorophenyl (like **2a**) or dichlorophenyl configurations (**2o**, **2p**, **2w**, and **2x**) had higher affinity than **2a** for all three targets, DAT, NET, and α3β4*-nAChR, implicated in **2a** action. The selectivity increase for **2a** analogues in blocking α3β4* nAChRs subtypes is very relevant, since these subtypes are highly expressed in the medial habenula and its primary target, the interpeduncular nucleus. Recent data suggest an important role for the habenulo-interpeduncular system and the nicotinic receptor subunits expressed therein in nicotine withdrawal.[28]

Seventeen of the analogues had higher potency than **2a** as antagonists of nicotine-induced antinociception in the tail-flick test, having AD_{50} values that ranged from ~2- to ~86-fold lower than that for **2a**. However, five analogues (**2d**, **2i**, **2l**, **2n**, and **2y**) were only slightly (~2-fold) better than **2a** as antagonists of nicotine-induced antinociception in the hot plate assay, just one analogue (**2d**) rivaled or bettered **2a** as an antagonist of nicotine's effects on locomotion, and only **2d**, **2i**, **2l**, and **2aa** rivaled or bettered the antagonistic potency of **2a** toward nicotine-induced hypothermia. Analogues **2m**, **2n**, and **2r** have the lowest AD_{50} values in the tail-flick assay, and yet only **2n** in the hot-plate assay shows any other form of nicotine

behavioral antagonism. Every ligand except **2p** that had higher potency than **2a** at α3β4*-nAChR also showed an improvement over **2a** in antagonistic potency in the tail-flick assay as did three of the ligands (**2o**, **2w**, and **2x** but not **2aa** and **2p**) that had higher potency than **2a** as antagonists for DA and NE uptake inhibition. Thus, increased potency at α3β4*-nAChR correlates with but is not necessary for improvement in ligand antagonist potency in the tail-flick assay. Moreover, when improvement in activity for DA and NE uptake inhibition is dissociated from improvement in activity at α3β4*-nAChR (i.e., for **2aa**), there is no improvement in behavioral antagonism in the tail-flick assay. Perhaps compounds like **2g**, **2i**, **2k**, **2j**, **2ff**, **3**, **4**, or even **2m**, **2n**, and **2r** that are not as active as **2a** in vitro are metabolized in vivo to forms that are active behaviorally and might also have higher affinity for DA and NE uptake inhibition and/or α3β4*-nAChR antagonism, but drug exposure times in vivo are short.

In summary, several **2a** analogues were synthesized and tested for their ability to inhibit monoamine uptake and to antagonize the effects of α3β4*, α4β2, α4β4, and α1β1 nAChRs. The analogues were also evaluated for their ability to block nicotine-induced antinociception, locomotor activity, and hypothermia. Analogues **2o**, **2p**, and **2x** had significantly better IC_{50} values for DA uptake inhibition relative to **2a**. Analogue **2x** also had a significantly better IC_{50} value for NE uptake inhibition relative to **2a**. Analogues **2l**, **2o**, **2p**, **2s**, **2w**, and **2x** had IC_{50} values of 2.6 to 3.6 times better than **2a** for the antagonism of the α3β4* nAChR. Seventeen of the **2a** analogues had better AD_{50} values for blocking nicotine-induced antinociception in the tail-flick test, with analogues **2m**, **2n**, and **2r** having the lowest AD_{50} values. Analogue **2x** with IC_{50} values of 31 and 180 nM for DA and NE uptake inhibition compared to 658 and 1850 nM for **2a** and an IC_{50} of 0.62 and 9.8 μM for antagonism of the α3β4* and α4β2 nAChRs, respectively, compared to 1.8 and 12 μM for **2a** had the best overall in vitro profile. This compound also had an AD_{50} of 0.13 mg/kg in the tail-flick test compared to an AD_{50} of 1.2 mg/kg for **2a**.

Overall, the findings support the idea that multiple molecular targets can play roles in mediating nicotine's behavioral effects and that these new **2a** analogues have potential not only as pharmacological tools to study targets and mechanisms involved but also as new pharmacotherapies with potentially higher efficacy as aids to smoking cessation.

Experimental Section

Chemistry. Nuclear magnetic resonance (^{1}H NMR and ^{13}C NMR) spectra were recorded on a 300 MHz (Bruker AVANCE 300) spectrometer. Chemical shift data for the proton resonances were reported in parts per million (δ) relative to internal $(CH_3)_4Si$ (δ 0.0). Optical rotations were measured on an AutoPol III polarimeter, purchased from Rudolf Research. Elemental analyses were performed by Atlantic Microlab, Norcross, GA. Purity of compounds (>95%) was established by elemental analysis. Analytical thin-layer chromatography (TLC) was carried out on plates precoated with silica gel GHLF (250 μM thickness). TLC visualization was accomplished with a UV lamp or in an iodine chamber. All moisture-sensitive reactions were performed under a positive pressure of nitrogen maintained by a direct line from a nitrogen source. Anhydrous solvents were purchased from Aldrich Chemical Co.

2-(*N*-*tert*-Butylamino)-3′-methoxypropiophenone (2e) Fumarate. To a stirred solution of 2-bromo-3′-methoxypropiophenone **7d** (400 mg, 1.5 mmol) in 3 mL of CH_3CN was added 0.315 mL (3.0 mmol) of *tert*-butyamine. The mixture was stirred for 10 h at room temperature. The reaction solution was diluted with EtOAc, washed with aqueous $NaHCO_3$, water, and brine, and then dried over Na_2SO_4. The solvent was evaporated, and the residue was purified by column chromatography on silica gel using MeOH−CH_2Cl_2 (1:50 to 1:10 w/ 1% NH_4OH) as the eluent to afford 138 mg (39%) of **2e**. The **2e** was immediately dissolved in Et_2O, 1.0 equiv of fumaric acid (dissolved in minimal amount of MeOH) was added dropwise, and the mixture was stirred overnight. The solid was collected by filtration, washed with Et_2O, and vacuum-dried to yield 150 mg (28%) of **2e** fumarate as a white solid: mp 152−153 °C. ^{1}H NMR (CD_3OD) δ 7.75 (d, J = 8.4 Hz, 1H), 7.63 (s, 1H), 7.54 (t, J = 8.1 Hz, 1H), 7.32 (dd, J = 8.0, 2.5 Hz, 1H), 6.68 (s, 2H), 5.20 (q, J = 7.1 Hz, 1H), 4.88 (s, 3H), 1.57 (d, J = 7.1 Hz, 3H), 1.35 (s, 9H). ^{13}C NMR (CD_3OD) δ 196.8, 170.8, 161.5, 135.7, 134.5, 131.2, 122.0, 114.2, 59.0, 55.7, 54.3, 26.2, 18.5. LCMS (ESI) m/z 236.5 $(M + 1)^+$. Anal. ($C_{18}H_{25}NO_6$) C, H, N.

2-(*N*-*tert*-Butylamino)-3′-nitropropiophenone (2f) Fumarate. To a stirred solution of 2-bromo-3′-nitropropiophenone **7e** (300 mg, 1.16 mmol) in 3 mL of CH_3CN was added *tert*-butyamine (0.170 g, 3.0 mmol). The mixture was stirred for 6 h at 40 °C. The solution was filtered to remove the white precipitate. The reaction solution was diluted with EtOAc, washed with aqueous $NaHCO_3$, water, and brine, and then dried over Na_2SO_4. The solvent was evaporated, and the residue was purified by column chromatography on silica gel using MeOH−CH_2Cl_2 (1:50 to 1:10 w/ 1% NH_4OH) as the eluent to afford 211 mg (73%) of **2f**. The **2f** was immediately dissolved in Et_2O, 1.0 equiv of fumaric acid (dissolved in minimal amount of MeOH) was added dropwise, and the mixture was stirred overnight. The solid was collected by filtration, washed with Et_2O, and vacuum-dried to give 270 mg (64% from **2f**) of **2f** fumarate as a white solid: mp 166−167 °C. ^{1}H NMR (CD_3OD) δ 8.94 (s, 1H), 8.59 (dd, 2H), 7.90 (t, 1H), 6.68 (s, 2H), 5.30 (q, 1H), 1.61 (d, 3H), 1.37 (s, 9H). ^{13}C NMR (CD_3OD) δ 198.5, 172.8, 152.1, 137.9, 137.5, 133.9, 131.9, 126.5, 60.9, 56.8, 29.5, 28.7, 20.6. LCMS (ESI) m/z 252.3 $(M + 1)^+$. Anal. ($C_{17}H_{22}N_2O_7$) C, H, N.

2-(*N*-Cyclopentylamino)-3′-fluoropropiophenone (2q) Hydrochloride. To a CH_3CN solution (3 mL) of 2-bromo-3′-fluoropropiophenone **7a** (290 mg, 1.26 mmol) was added cyclopentylamine (125 μL, 1.26 mmol), and the mixture was allowed to react for 3 h at room temperature. The precipitate was filtered off. The filtrate was concentrated, and the residue was purified by column chromatography on silica gel using cyclohexane−EtOAc (2:1 to 1:0 with 1% NH_4OH) as the eluent to give **2q** as a light-yellow oil. The **2q** was dissolved in 50 mL of Et_2O, a solution of hydrochloric acid in Et_2O was added dropwise, and the mixture was stirred overnight. The precipitate was filtered, washed with Et_2O, and dried under vacuum to give 50 mg (15%) of **2q**·HCl as a white solid: mp 185−186 °C. ^{1}H NMR (CD_3OD) δ 7.95 (d, 1H), 7.85 (d, 1H), 7.64 (m, 1H), 7.51 (m, 1H), 5.16 (m, 1H), 3.64 (m, 1H), 2.15 (m, 2H), 1.61−1.85 (m, 6H), 1.60 (d, 3H). ^{13}C NMR (CD_3OD) δ 196.4, 166.5, 163.2, 136.8, 136.7, 133.0, 126.6, 123.5, 123.2, 117.0, 116.7, 59.2, 58.9, 31.2, 25.2, 17.0. LCMS (ESI) m/z 236.4 $(M + 1)^+$. Anal. ($C_{14}H_{19}ClFNO$) C, H, N.

2-(*N*-Cyclopentylamino)-3′-bromopropiophenone (2s) Fumarate. To a CH_3CN solution (5 mL) of 2-bromo-3′-bromopropiophenone **7b** (480 mg, 1.65 mmol) was added cyclopentylamine (330 μL, 3.31 mmol), and the mixture was allowed to react for 6 h at 40 °C. After the mixture was cooled to room temperature, the precipitate was removed by filtration. The filtrate was concentrated, and the residue was purified by column chromatography on silica gel using cyclohexane−EtOAc (2:1 to 1:0 with 1% NH_4OH) as the eluent to give 182 mg (37%) of **2s** as light-yellow oil. The **2s** was dissolved in 50 mL of Et_2O, a MeOH solution (1 mL) of fumaric acid (71 mg) was added dropwise, and the mixture was stirred overnight. The precipitate was collected, washed with Et_2O, and dried under vacuum to give 240 mg (35%) of **2s** fumarate as a white solid: mp 152−153 °C. ^{1}H NMR (CD_3OD) δ 8.25 (s, 1H), 8.07 (d, 1H), 7.89 (d, 1H), 7.54 (t, 1H), 6.68 (s, 2H), 5.13 (q, 1H),

3.30 (m, 1H), 2.13 (m, 2H), 1.83 (m, 2H), 1.68 (m, 4H), 1.56 (d, 3H). ^{13}C NMR (CD_3OD) δ 196.8, 171.6, 139.2, 136.7, 136.6, 133.1, 132.6, 129.2, 124.8, 59.2, 59.2, 32.5, 31.3, 25.2, 17.2, 14.8. LCMS (ESI) m/z 296.2 $(M + 1)^+$. Anal. ($C_{18}H_{22}BrNO_5$) C, H, N.

2-(*N*-Cyclopentylamino)-3′-methylpropiophenone (2t) Fumarate. To a CH_3CN solution (4 mL) of 2-bromo-3′-methylpropiophenone **7c** (400 mg, 1.76 mmol) was added cyclopentylamine (175 μL, 1.76 mmol), and the mixture was allowed to react for 6 h at 40 °C. After the mixture was cooled to room temperature, the precipitate was filtered off. The filtrate was concentrated, and the residue was purified by column chromatography on silica gel using cyclohexane−EtOAc (2:1 to 1:0 with 1% NH_4OH) as the eluent to give 226 mg (56%) of **2t** as light-yellow oil. The free base was dissolved in 50 mL of Et_2O, MeOH solution (1 mL) of fumaric acid (1 equiv) was added dropwise, and the mixture was stirred overnight. The precipitate was collected, washed with Et_2O, and dried under vacuum to give 260 mg (43%) of **2t** fumarate as a white solid: mp 171−172 °C. ^{1}H NMR (CD_3OD) δ 7.90 (m, 2H), 7.56 (d, J = 7.5 Hz, 1H), 7.48 (t, J = 7.6 Hz, 1H), 6.68 (s, 2H), 5.14 (q, J = 7.1 Hz, 1H), 3.59 (m, 1H), 2.45 (s, 3H), 2.13 (m, 2H), 1.90−1.65 (m, 6H), 1.58 (d, J = 7.1 Hz, 3H). ^{13}C NMR (CD_3OD) δ 201.0, 175.1, 144.4, 140.5, 139.9, 138.1, 134.0, 130.9, 62.6, 61.9, 34.5, 28.6, 25.0, 20.7, 10.8. LCMS (ESI) m/z 232.8 $(M + 1)^+$. Anal. ($C_{19}H_{25}NO_5$) C, H, N.

2-(*N*-Cyclopentylamino)-3′-methoxypropiophenone (2u) Fumarate. To a CH_3CN solution (6 mL) of 2-bromo-3′-methoxypropiophenone **7d** (600 mg, 2.47 mmol) was added cyclopentylamine (245 μL, 2.47 mmol), and the mixture was allowed to react for 6 h at 40 °C. After the mixture was cooled to room temperature, the precipitate was filtered off. The filtrate was concentrated, and the residue was purified by column chromatography on silica gel using cyclohexane−EtOAc (2:1 to 1:0 with 1% NH_4OH) as the eluent to give **2u** as a light-yellow oil. The **2u** was dissolved in 50 mL of Et_2O, and a MeOH solution (1 mL) of fumaric acid (1 equiv) was added dropwise and stirred overnight. The precipitate was collected, washed with Et_2O, and dried under vacuum to give 290 mg (33%) of **2u** fumarate as an off-white solid: mp 144−145 °C. ^{1}H NMR (DMSO-d_6) δ 7.66 (d, J = 7.7 Hz, 1H), 7.50 (m, 2H), 7.27 (dd, J = 8.2, 2.4 Hz, 1H), 6.53 (s, 2H), 4.72 (m, 1H), 3.84 (s, 3H), 3.18 (m, 1H), 1.77 (m, 2H), 1.64 (m, 2H), 1.48 (m, 4H), 1.29 (d, J = 6.9 Hz, 3H). ^{13}C NMR (CD_3OD) δ 196.5, 170.7, 161.3, 135.6, 135.1, 131.0, 121.8, 121.5, 113.9, 58.3, 57.7, 55.5, 30.3, 24.3, 16.4. LCMS (ESI) m/z 248.3 $(M + 1)^+$. Anal. ($C_{19}H_{25}NO_6$) C, H, N.

2-(*N*-Cyclopentylamino)-3′-nitropropiophenone (2v) Hydrochloride. To a CH_3CN solution (3 mL) of 2-bromo-3′-nitropropiophenone **7e** (300 mg, 1.16 mmol) was added cyclopentylamine (230 μL, 2.32 mmol), and the mixture was allowed to react for 6 h at room temperature. The precipitate was filtered off. The filtrate was concentrated, and the residue was purified by column chromatography on silica gel using cyclohexane−EtOAc (2:1 to 1:0 with 1% NH_4OH) as the eluent to give **2v** as a light-yellow oil. The **2v** was dissolved in 50 mL of Et_2O, a solution of hydrochloric acid in Et_2O was added dropwise, and the mixture was stirred overnight. The precipitate was collected, washed with Et_2O, and dried under vacuum to give 50 mg (15%) of **2v**·HCl as a white solid: mp 149−150 °C. ^{1}H NMR (CD_3OD) δ 8.88 (s, 1H), 8.60 (s, 1H), 8.51 (s, 1H), 7.89 (s, 1H), 5.28 (s, 1H), 3.68 (s, 1H), 2.19 (s, 2H), 1.64−1.87 (m, 9H). ^{13}C NMR (CD_3OD) δ 195.6, 150.4, 135.9, 135.6, 132.2, 130.1, 124.7, 59.0, 58.8, 31.0, 25.0, 16.7. Anal. ($C_{17}H_{19}ClN_2O_3 \cdot 0.5H_2O$) C, H, N.

2-(*N*-Pyrrolidinyl)-3′-fluoropropiophenone (2aa) Hydrochloride. To a CH_3CN solution (3 mL) of 2-bromo-3′-fluoropropiophenone **7a** (300 mg, 1.30 mmol) was added pyrrolidine (108 μL, 1.30 mmol), and the mixture was allowed to react for 3 h at room temperature. The precipitate was filtered off. The filtrate was concentrated, and the residue was purified by column chromatography on silica gel using cyclohexane−EtOAc (2:1 to 1:0 with 1% NH_4OH) as the eluent to give the **2aa** as a light-yellow oil. The **2aa** was dissolved in Et_2O, a solution of hydrochloric acid in Et_2O was added dropwise, and the mixture was stirred overnight. The precipitate was collected, washed with Et_2O, and dried under vacuum to give 180 mg (54%) of **2aa**·HCl as a white solid: mp 184−185 °C. ^{1}H NMR (CD_3OD) δ 7.91 (d, 1H), 7.81 (d, 1H), 7.64 (m, 1H), 7.52 (m, 1H), 5.32 (m, 1H), 3.73 (m, 2H), 3.07 (m, 2H), 2.09−2.16 (m, 4H), 1.63 (d, 3H). ^{13}C NMR (CD_3OD) δ 196.3, 166.2, 162.9, 136.5, 132.7, 132.6, 126.2, 123.3, 123.1, 116.7, 116.4, 66.9, 55.8, 53.4, 24.4, 16.8. LCMS (ESI) m/z 222.6 $(M + 1)^+$. Anal. ($C_{13}H_{17}ClFNO$) C, H, N.

2-(*N*-Pyrrolidinyl)-3′-bromopropiophenone (2bb) Fumarate. To a CH_3CN/H_2O solution (4 mL/2 mL) of 2-bromo-3′-bromopropiophenone **7b** (700 mg, 2.4 mmol) was added pyrrolidine (200 μL, 2.4 mmol), and the mixture was allowed to react for 4 h at room temperature. The reaction solution was diluted with EtOAc, washed with aqueous $NaHCO_3$, water, and brine, and then dried over Na_2SO_4. The solvent was evaporated, and the residue was purified by column chromatography on silica gel using cyclohexane−EtOAc (2:1 to 1:0 with 1% NH_4OH) as the eluent to give 452 mg (67%) of **2bb** as a light-yellow oil. The **2bb** was dissolved in 50 mL of Et_2O, a MeOH solution (1 mL) of fumaric acid (1 equiv) was added dropwise, and the mixture was stirred overnight. The precipitate was collected, washed with Et_2O, and dried under vacuum to give **2bb** fumarate as a white solid: mp 134−135 °C. ^{1}H NMR ($CDCl_3$) δ 8.25 (s, 1H), 8.05 (d, 1H), 7.67 (d, 1H), 7.33 (t, 1H), 3.91 (q, 1H), 2.61 (m, 4H), 1.80 (m, 4H), 1.37 (d, 9H). ^{13}C NMR ($CDCl_3$) δ 199.7, 137.8, 135.8, 131.8, 130.1, 127.3, 122.8, 65.0, 51.1, 23.6, 15.8. LCMS (ESI) m/z 284.7 $(M + 1)^+$. Anal. ($C_{17}H_{20}BrNO_5$) C, H, N.

2-(*N*-Pyrrolidinyl)-3′-methylpropiophenone (2cc) Fumarate. To a CH_3CN-H_2O solution (4 mL-2 mL) of 2-bromo-3′-methylpropiophenone **7c** (400 mg, 1.76 mmol) was added pyrrolidine (150 μL, 1.76 mmol), and the mixture was allowed to react for 4 h at room temperature. The reaction solution was diluted with EtOAc, washed with aqueous $NaHCO_3$, water, and brine, and then dried over Na_2SO_4. The solvent was evaporated, and the residue was purified by column chromatography on silica gel using cyclohexane−EtOAc (2:1 to 1:0 with 1% NH_4OH) as the eluent to give **2cc** as a light-yellow oil. The **2cc** was dissolved in Et_2O, a MeOH solution (1 mL) of fumaric acid (1 equiv) was added dropwise, and the mixture was stirred overnight. The precipitate was collected, washed with Et_2O, and dried under vacuum to give 320 mg (55%) of **2cc** fumarate as a white solid: mp 131−132 °C. ^{1}H NMR (CD_3OD) δ 7.86 (m, 2H), 7.57 (d, J = 7.6 Hz, 1H), 7.48 (t, J = 7.6 Hz, 1H), 6.69 (s, 2H), 5.23 (q, J = 7.1 Hz, 1H), 3.55−3.33 (m, 4H), 2.45 (s, 3H), 2.12 (m, 4H), 1.60 (d, J = 7.1 Hz, 3H). ^{13}C NMR (CD_3OD) δ 201.2, 175.0, 144.4, 140.6, 139.9, 138.2, 134.0, 130.9, 70.3, 58.0, 28.0, 25.0, 20.6. LCMS (ESI) m/z 218.1 $(M + 1)^+$. Anal. ($C_{18}H_{23}NO_5$) C, H, N.

2-(*N*-Pyrrolidinyl)-3′-methoxypropiophenone (2dd) Fumarate. To a CH_3CN-H_2O solution (4 mL/2 mL) of 2-bromo-3′-methyoxypropiophenone **7d** (600 mg, 2.47 mmol) was added pyrrolidine (200 μL, 2.4 mmol), and the mixture was allowed to react for 4 h at room temperature. The reaction solution was diluted with EtOAc, washed with aqueous $NaHCO_3$, water, and brine, and then dried over Na_2SO_4. The solvent was evaporated, and the residue was purified by column chromatography on silica gel using cyclohexane−-EtOAc (2:1 to 1:0 with 1% NH_4OH) as the eluent to give 300 mg (52%) of **2dd** as a light-yellow oil. The **2dd** was dissolved in 50 mL of Et_2O, a MeOH solution (1 mL) of fumaric acid (1 equiv) was added dropwise, and the mixture was stirred overnight. The precipitate was collected, washed with Et_2O, and dried under vacuum to give 340 mg (39%) of **2dd** fumarate as a white solid: mp 121−122 °C. ^{1}H NMR (DMSO-d_6) δ 7.67 (d, J = 7.7 Hz, 1H), 7.56 (s, 1H), 7.47 (t, J = 8.1 Hz, 1H), 7.24 (dd, J = 8.2, 2.6 Hz, 1H), 6.58 (s, 2H), 4.46 (m, 1H), 3.82 (s, 3H), 2.76 (s, 4H), 1.74 (s, 4H), 1.29 (d, J = 6.8 Hz, 3H). ^{13}C NMR (DMSO-d_6) δ 197.7, 165.0, 157.8, 135.0, 132.7, 128.3, 119.4, 117.8, 111.6, 61.2, 53.7, 48.6, 21.6, 12.8. LCMS (ESI) m/z 234.3 $(M + 1)^+$. Anal. ($C_{18}H_{23}NO_6$) C, H, N.

2-(*N*-Pyrrolidinyl)-3′-nitropropiophenone (2ee) Hydrochloride. To a CH_3CN-H_2O solution (4 mL/2 mL) of **7e** (310 mg, 1.2 mmol) was added pyrrolidine (100 μL, 1.2 mmol), and the mixture was allowed to react for 2 h at room temperature. The reaction solution was diluted with EtOAc, washed with aqueous $NaHCO_3$, water, and brine, and then dried over Na_2SO_4. The solvent was evaporated, and the residue was purified by column chromatography on silica gel using cyclohexane−EtOAc (2:1 to 1:0 with 1% NH_4OH) as the eluent to give 120 mg (40%) of **2ee** as a light-yellow oil. The **2ee** was dissolved in 50 mL of Et_2O, a solution of hydrochloric acid in ether was added dropwise, and the mixture was stirred overnight. The precipitate was collected, washed with Et_2O, and dried under vacuum to give 60 mg (18%) of **2ee**·HCl as an off-white solid: mp 35−36 °C. ^{1}H NMR (CD_3OD) δ 8.86 (s, 1H), 8.59 (s, 1H), 8.50 (s, 1H), 7.91 (s, 1H), 5.50 (s, 1H), 3.80 (s, 2H), 3.40 (m, 2H), 2.14 (m, 4H), 1.70 (s, 3H). ^{13}C NMR (CD_3OD) δ 196.2, 150.7, 136.8, 136.1, 132.9, 130.6, 125.3, 67.9, 56.8, 54.6, 25.3, 25.2, 17.7. LCMS (ESI) m/z 249.2 $(M + 1)^+$. Anal. ($C_{13}H_{17}ClN_2O_3 \cdot H_2O$) C, H, N.

General Procedure for 2-Bromo-3-Substituted Propiophenones 7a−e. To a solution of the appropriate propiophenone **6a−e** (25 mmol) in acetic acid (45 mL), bromine (25 mmol) was added dropwise. After the mixture was stirred overnight, the acetic acid was removed under vacuum, and the resulting residue was dissolved in EtOAc, washed with saturated $NaHCO_3$ solution, brine, dried (Na_2SO_4), and concentrated to give the bromoketones **7a−e**. The unpurified **7a−e** were used to prepare the **2a** analogues without further purification.

Cell Lines and Culture. HEK-293 cells stably expressing human DAT, NET, or SERT were maintained as previously described.[26] Use was made of several human cell lines that naturally or heterologously express specific, functional, human nAChR subtypes.[29] Cells of the TE671/RD line naturally expresses muscle-type nAChR ($\alpha1\beta1\gamma\delta$- or $\alpha1$*-nAChR), and SH-SY5Y neuroblastoma cells naturally expresses autonomic $\alpha3\beta4$*-nAChRs (containing $\alpha3$, $\beta4$, probably $\alpha5$, and sometimes $\beta2$ subunits). Different clones of SH-EP1 epithelial cell lines have been engineered to heterologously express either $\alpha4\beta2$-nAChR, which is thought to be the most abundant, high affinity nicotine-binding nAChR in mammalian brain, or $\alpha4\beta4$-nAChR, another possible brain nAChR subtype (SH-EP1-h$\alpha4\beta2$ or $\alpha4\beta4$ cells, respectively).[30,31] These cells were maintained as low passage number (1−26 from our frozen stocks) cultures to ensure stable expression of native or heterologously expressed nAChR as previously described.[29] Cells were passaged once weekly by splitting just-confluent cultures 1/300 (TE671/RD), 1/5 (SH-SY5Y), or 1/20 (transfected SH-EP1) in serum-supplemented medium to maintain log-phase growth.

Transporter Assays. The abilities of **2a** and its analogues to inhibit uptake of [^{3}H]dopamine ([^{3}H]DA), [^{3}H]serotonin ([^{3}H]5-HT), or [^{3}H]norepinephrine ([^{3}H]NE) by the respective human transporters were evaluated using the appropriate HEK-293 cell line as previously reported.[26]

nAChR Functional Assays. Cells were harvested at confluence from 100 mm plates by mild trypsinization (Irvine Scientific, Santa Ana, CA) and trituration or (for SH-SY5Y cells) by trituration alone before being suspended in complete medium and evenly seeded at a density of 1.25−2 confluent 100 mm plates per 24-well plate (Falcon; ∼100−125 μg of total cell protein per well in a 500 μL volume). After cells had adhered (generally overnight but no sooner than 4 h later), the medium was removed and replaced with 250 μL per well of complete medium supplemented with ∼350000 cpm of $^{86}Rb^+$ (PerkinElmer Life and Analytical Sciences, Boston, MA) and counted at 40% efficiency using Cerenkov counting (TriCarb 1900 liquid scintillation analyzer, 59% efficiency; PerkinElmer Life Sciences). After at least 4 h and typically overnight, $^{86}Rb^+$ efflux was measured using the "flip-plate" technique.[29] Briefly, after aspiration of the bulk of $^{86}Rb^+$ loading medium from each well of the "cell plate", each well containing cells was rinsed 3× with 2 mL of fresh $^{86}Rb^+$ efflux buffer (130 mM NaCl, 5.4 mM KCl, 2 mM $CaCl_2$, 5 mM glucose, 50 mM HEPES, pH 7.4) to remove extracellular $^{86}Rb^+$. Following removal of residual rinse buffer by aspiration, the flip-plate technique was used again to simultaneously introduce 1.5 mL of fresh efflux buffer containing drugs of choice at indicated final concentrations from a 24-well "efflux/drug plate" into the wells of the cell plate. After a 5 min incubation, the solution was "flipped" back into the efflux/drug plate, and any remaining buffer in the cell plate was removed by aspiration. Cells remaining in the cell plate were lysed and suspended by addition of 1.5 mL of 0.1 M NaOH, 0.1% sodium dodecyl sulfate to each well. Suspensions in each well were then subjected to Cerenkov counting (Wallac Micobeta Trilux 1450; 25% efficiency) after placement of inserts (Wallac 1450−109) into each well to minimize cross-talk between wells.

For quality control and normalization purposes, the sum of $^{86}Rb^+$ in cell plates and efflux/drug plates was defined to confirm material balance (i.e., that the sum of $^{86}Rb^+$ released into the efflux/drug plates and $^{86}Rb^+$ remaining in the cell plate was the same for each well). This ensured that $^{86}Rb^+$ efflux was the same whether measured in absolute terms or as a percentage of loaded $^{86}Rb^+$. Similarly, the sum of $^{86}Rb^+$ in cell plates and efflux/drug plates also determined the efficiency of $^{86}Rb^+$ loading (the percentage of applied $^{86}Rb^+$ actually loaded into cells).

Control, total $^{86}Rb^+$ efflux was assessed in the presence of only a fully efficacious concentration of carbamylcholine (1 mM for SH-EP1-h$\alpha4\beta2$, SH-EP1-h$\alpha4\beta4$ cells or TE671/RD cells; 3 mM for SH-SY5Y cells). Control, nonspecific $^{86}Rb^+$ efflux was measured either in the presence of the fully efficacious concentration of carbamylcholine plus 100 μM mecamylamine, which gave full block of agonist-induced and spontaneous nAChR-mediated ion flux, or in the presence of efflux buffer alone. Either determination of nonspecific efflux was equivalent. Specific efflux was then taken as the difference in control samples between total and nonspecific $^{86}Rb^+$ efflux. Any intrinsic agonist activity of test drugs was ascertained using samples containing test drug only at different concentrations and was normalized, after subtraction of nonspecific efflux, to specific efflux in test drug-free, control samples. Antagonism of carbamylcholine-evoked $^{86}Rb^+$ efflux was assessed in samples containing the full agonist at a concentration where it stimulates 80−90% of maximal function (i.e., its $EC_{80}-EC_{90}$ value) when exposed alone to a given nAChR subtype (i.e, 460 μM for TE671/RD cells, 2 mM for SH-SY5Y cells, 200 μM for SH-EP1-h$\alpha4\beta2$ or -$\alpha4\beta4$ cells) and test drugs at the concentrations shown. After subtraction of nonspecific efflux, results were normalized to specific ion flux in control samples. For studies of mechanism of antagonism, concentration−response curves were obtained using samples containing the full agonist, carbamylcholine, at the indicated concentrations alone or in the presence of a concentration of the test ligand close to its IC_{50} value for inhibition of nAChR function. In other studies, cells were pre-exposed to analogues for 1 h (over the last hour of $^{86}Rb^+$ loading) or 1 day (with $^{86}Rb^+$ loading occurring during the final 4 h of drug pretreatment) before effects on nAChR function were assessed after analogue was removed (during extracellular $^{86}Rb^+$ removal) or in the continued presence of drug.

Ion flux assay results were fit using Prism (GraphPad) to the Hill equation, $F = F_{max}/(1 + (X/Z)^n)$, where F is the test sample specific ion flux as a percentage of control, F_{max} is specific ion flux in the absence of test drug (i.e., for control samples), X is the test ligand concentration, Z is the EC_{50} ($n > 0$ for agonists) or IC_{50} ($n < 0$ for antagonists), and n is the Hill coefficient. All concentration−ion flux response curves were simple and fit well, allowing maximum and minimum ion flux values to be determined by curve fitting, but in cases where antagonists had weak functional potency, minimum ion flux was set at 0% of control. Note that because agonist concentrations used for test ligand antagonism assessments were $EC_{80}-EC_{90}$ values, not all of the data, even at the lowest concentrations of test antagonist, approach 100% of specific efflux, as separately determined in

sister samples exposed to fully efficacious concentrations of agonist.

Behavior. All animal experiments were conducted in accordance with the NIH Guide for the Care and Use of Laboratory Animals and Institutional Animal Care and Use Committee guidelines.

Animals. Male Institute of Cancer Research (ICR) mice (weighing 20−25 g) obtained from Harlan (Indianapolis, IN) were used throughout the study. Animals were housed in an Association for Assessment and Accreditation of Laboratory Animal Care approved facility, were placed in groups of six, and had free access to food and water. Studies were approved by the Institutional Animal Care and Use Committee of Virginia Commonwealth University.

Tail-Flick Test. Antinociception for pain mediated at the spinal level was assessed by the tail-flick method of D'Amour and Smith.[32] In brief, mice were lightly restrained while a radiant heat source was shone onto the upper portion of the tail. To minimize tissue damage, a maximum latency of 10 s was imposed. Latency to remove the tail from the heat source was recorded for each animal. A control response (2−4 s) was determined for each mouse before treatment, and a test latency was determined after drug administration (nicotine as an analgesic 5 min after subcutaneous administration at 2.5 mg/kg; nicotine administration 15 min after exposure to saline of **2a** analogue to assess the latter drug's ability to block nicotine-mediated antinociception). Antinociceptive response was calculated as the percentage of maximum possible effect (%MPE), where %MPE = [(test control)/(10 control)] × 100.

Hot-Plate Test. Mice were placed into a 10 cm wide glass cylinder on a hot plate (Thermojust Apparatus) maintained at 55 °C for assessment of pain responses mediated at supraspinal levels. To minimize tissue damage, a maximum exposure to the hot plate of 40 s was imposed. Measures of control latencies (time until the animal jumped or licked its paws; typically 8−12 s) were done twice for stimuli applied at least 10 min apart for each mouse. Antinociceptive responses after test drug administrations were determined and calculated as the %MPE, where %MPE = [(test latency in s − control latency in s)/(40 s − controllatency in s) × 100]. Groups of 8−12 animals were used for each drug condition. Antagonism studies were carried in mice pretreated with either saline or **2a** metabolites 15 min before nicotine. The animals were then tested 5 min after administration of a subcutaneous dose of 2.5 mg/kg nicotine.

Locomotor Activity. Mice were placed into individual Omnitech photocell activity cages (28 cm × 16.5 cm; Omnitech Electronics, Columbus, OH) 5 min after subcutaneous administration of either 0.9% saline or nicotine (1.5 mg/kg). Interruptions of the photocell beams (two banks of eight cells each) were then recorded for the next 10 min. Data were expressed as the number of photocell interruptions. Antagonism studies were carried out by pretreating the mice with either saline or **2a** metabolites 15 min before nicotine.

Body Temperature. Rectal temperature was measured by a thermistor probe (inserted 24 mm) and digital thermometer (YSI Inc., Yellow Springs, OH). Readings were taken just before and 30 min after subcutaneous injection of either saline or 2.5 mg/kg nicotine. The difference in rectal temperature before and after treatment was calculated for each mouse. The ambient temperature of the laboratory varied from 21 to 24 °C from day to day. Antagonism studies were carried out by pretreating the mice with either saline or **2a** metabolites 15 min before nicotine. The animals were then tested 30 min after administration of a subcutaneous dose of 2.5 mg/kg nicotine.

Acknowledgment. This work was supported by National Institutes of Health National Cooperative Drug Discovery Group Grant U19 DA019377. Other effort was supported by grants (to R.J.L) from the National Institutes of Health (Grant DA015389) and the Barrow Neurological Foundation.

Supporting Information Available: Results from elemental analysis. This material is available free of charge via the Internet at http://pubs.acs.org.

References

(1) *WHO Report on the Global Tobacco Epidemic, 2008: The MPOWER Package*; World Health Organization: Geneva, 2008; p 15.
(2) Centers for Disease Control and Prevention. Cigarette smoking among adults: United States, 2007. *Morbidity Mortality Wkly. Rep.* **2007**, *56*, 1157−1161.
(3) Benowitz, N. L. Clinical pharmacology of nicotine: implications for understanding, preventing, and treating tobacco addiction. *Clin. Pharmacol. Ther.* **2008**, *83*, 531–541.
(4) Lerman, C.; LeSage, M. G.; Perkins, K. A.; O'Malley, S. S.; Siegel, S. J.; Benowitz, N. L.; Corrigall, W. A. Translational research in medication development for nicotine dependence. *Nat. Rev. Drug Discovery* **2007**, *6*, 746–762.
(5) Gotti, C.; Moretti, M.; Gaimarri, A.; Zanardi, A.; Clementi, F.; Zoli, M. Heterogeneity and complexity of native brain nicotinic receptors. *Biochem. Pharmacol.* **2007**, *74*, 1102–1111.
(6) Rahman, S.; Lopez-Hernandez, G. Y.; Corrigall, W. A.; Papke, R. L. Neuronal nicotinic receptors as brain targets for pharmacotherapy of drug addiction. *CNS Neurol. Disord.: Drug Targets* **2008**, *7*, 422–441.
(7) Adams, D. J.; Nutter, T. J. Calcium permeability and modulation of nicotinic acetylcholine receptor-channels in rat parasympathetic neurons. *J. Physiol.* (*Paris*) **1992**, *86*, 67–76.
(8) Le Novere, N.; Zoli, M.; Changeux, J. P. Neuronal nicotinic receptor alpha 6 subunit mRNA is selectively concentrated in catecholaminergic nuclei of the rat brain. *Eur. J. Neurosci.* **1996**, *8*, 2428–2439.
(9) Goldner, F. M.; Dineley, K. T.; Patrick, J. W. Immunohistochemical localization of the nicotinic acetylcholine receptor subunit alpha6 to dopaminergic neurons in the substantia nigra and ventral tegmental area. *NeuroReport* **1997**, *8*, 2739–2742.
(10) Exley, R.; Clements, M. A.; Hartung, H.; McIntosh, J. M.; Cragg, S. J. Alpha6-containing nicotinic acetylcholine receptors dominate the nicotine control of dopamine neurotransmission in nucleus accumbens. *Neuropsychopharmacology* **2008**, *33*, 2158–2166.
(11) Corrigall, W. A.; Franklin, K. B.; Coen, K. M.; Clarke, P. B. The mesolimbic dopaminergic system is implicated in the reinforcing effects of nicotine. *Psychopharmacology* **1992**, *107*, 285–289.
(12) Brody, A. L.; Olmstead, R. E.; London, E. D.; Farahi, J.; Meyer, J. H.; Grossman, P.; Lee, G. S.; Huang, J.; Hahn, E. L.; Mandelkern, M. A. Smoking-induced ventral striatum dopamine release. *Am. J. Psychiatry* **2004**, *161*, 1211–1218.
(13) Fant, R. V.; Buchhalter, A. R.; Buchman, A. C.; Henningfield, J. E. Pharmacotherapy for Tobacco Dependence. In *Nicotine Psychopharmacology. Handbook of Experimental Pharmacology*; Henningfield, J. E., London, E. D., Pogun, S., Eds.; Springer-Verlag: Berlin, 2009; Vol. 192, p 487.
(14) Gonzales, D.; Rennard, S. I.; Nides, M.; Oncken, C.; Azoulay, S.; Billing, C. B.; Watsky, E. J.; Gong, J.; Williams, K. E.; Reeves, K. R. Varenicline, an alpha4beta2 nicotinic acetylcholine receptor partial agonist, vs sustained-release bupropion and placebo for smoking cessation: a randomized controlled trial. *JAMA, J. Am. Med. Assoc.* **2006**, *296*, 47–55.
(15) Fryer, J. D.; Lukas, R. J. Noncompetitive functional inhibition at diverse, human nicotinic acetylcholine receptor subtypes by bupropion, phencyclidine, and ibogaine. *J. Pharmacol. Exp. Ther.* **1999**, *288*, 88–92.
(16) Slemmer, J. E.; Martin, B. R.; Damaj, M. I. Bupropion is a nicotinic antagonist. *J. Pharmacol. Exp. Ther.* **2000**, *295*, 321–327.
(17) Harbeson, S. L. Propiophenone Derivatives. WIPO Patent WO/2009/105218, **2009**.
(18) Hadizadeh, F.; Ebrahimzadeh, M. A.; Hosseinzadeh, H.; Motamed-Shariaty, V.; Salami, S.; Bekhradnia, A. R. Antidepressant and antioxidant activities of some 2-benzoxazolinone derivatives as bupropion analogues. *Pharmacologyonline* **2009**, *1*, 331–335.
(19) Foley, K. F.; Cozzi, N. V. Novel aminopropiophenones as potential antidepressants. *Drug Dev. Res.* **2003**, *60*, 252–260.
(20) Miller, D. K.; Sumithran, S. P.; Dwoskin, L. P. Bupropion inhibits nicotine-evoked [(3)H]overflow from rat striatal slices preloaded with [(3)H]dopamine and from rat hippocampal slices preloaded with [(3)H]norepinephrine. *J. Pharmacol. Exp. Ther.* **2002**, *302*, 1113–1122.

(21) Mooney, M. E.; Sofuoglu, M. Bupropion for the treatment of nicotine withdrawal and craving. *Expert Rev. Neurother.* **2006**, *6*, 965–981.
(22) Paterson, N. E.; Balfour, D. J.; Markou, A. Chronic bupropion attenuated the anhedonic component of nicotine withdrawal in rats via inhibition of dopamine reuptake in the nucleus accumbens shell. *Eur. J. Neurosci.* **2007**, *25*, 3099–3108.
(23) Reuben, M.; Boye, S.; Clarke, P. B. Nicotinic receptors modulating somatodendritic and terminal dopamine release differ pharmacologically. *Eur. J. Pharmacol.* **2000**, *393*, 39–49.
(24) Makhay, M. M.; O'Donnell, J. M. Effects of antidepressants in rats trained to discriminate the beta-2 adrenergic agonist clenbuterol. *Pharmacol., Biochem. Behav.* **1999**, *63*, 319–324.
(25) Carroll, F. I.; Blough, B.; Abraham, P.; Mills, A. C.; Holleman, J. A.; Wolckenhauer, S. A.; Decker, A. M.; Landavazo, A.; McElroy, K. T.; Navarro, H. A.; Gatch, M. B.; Foster, M. J. Synthesis and biological evaluation of bupropion analogues as potential pharmacotherapies for cocaine addiction. *J. Med. Chem.* **2009**, *52*, 6768–6781.
(26) Eshleman, A. J.; Carmolli, M.; Cumbay, M.; Martens, C. R.; Neve, K. A.; Janowsky, A. Characteristics of drug interactions with recombinant biogenic amine transporters expressed in the same cell type. *J. Pharmacol. Exp. Ther.* **1999**, *289*, 877–885.
(27) Damaj, M. I.; Carroll, F. I.; Eaton, J. B.; Navarro, H. A.; Blough, B. E.; Mirza, S.; Lukas, R. J.; Martin, B. R. Enantioselective effects of hydroxy metabolites of bupropion on behavior and on function of monoamine transporters and nicotinic receptors. *Mol. Pharmacol.* **2004**, *66*, 675–682.
(28) Salas, R.; Sturm, R.; Boulter, J.; De Biasi, M. Nicotinic receptors in the habenulo-interpeduncular system are necessary for nicotine withdrawal in mice. *J. Neurosci.* **2009**, *29*, 3014–3018.
(29) Lukas, R. J.; Fryer, J. D.; Eaton, J. B.; Gentry, C. L. Some Methods for Studies of Nicotinic Acetylcholine Receptor Pharmacology. In *Nicotinic Receptors and the Nervous System*; Levin, E. D., Ed.; CRC Press: Boca Raton, FL, 2002; pp 3−27.
(30) Eaton, J. B.; Peng, J. H.; Schroeder, K. M.; George, A. A.; Fryer, J. D.; Krishnan, C.; Buhlman, L.; Kuo, Y. P.; Steinlein, O.; Lukas, R. J. Characterization of human alpha 4 beta 2-nicotinic acetylcholine receptors stably and heterologously expressed in native nicotinic receptor-null SH-EP1 human epithelial cells. *Mol. Pharmacol.* **2003**, *64*, 1283–1294.
(31) Gentry, C. L.; Lukas, R. J. Local anesthetics noncompetitively inhibit function of four distinct nicotinic acetylcholine receptor subtypes. *J. Pharmacol. Exp. Ther.* **2001**, *299*, 1038–1048.
(32) D'Amour, F. E.; Smith, D. L. A method for determining loss of pain sensation. *J. Pharmacol. Exp. Ther.* **1941**, *72*, 74–79.